

1 **100 Ma cycles of oceanic lithosphere generation in peri-Gondwana:**
2 **Neoproterozoic to Devonian ophiolites from the NW African-Iberian**
3 **margin of Gondwana and the Variscan Orogen**

4
5 Ricardo Arenas^{1*}, Sonia Sánchez Martínez¹, Richard Albert², Faouziya Haissen³,
6 Javier Fernández-Suárez¹, Núria Pujol-Solà⁴, Pilar Andonaegui¹,
7 Rubén Díez Fernández⁵, Joaquín A. Proenza⁴, Antonio Garcia-Casco⁶ &
8 Axel Gerdes²

9
10 *¹Departamento de Mineralogía y Petrología and Instituto de Geociencias (UCM, CSIC),*
11 *Universidad Complutense. 28040 Madrid, Spain.*

12 *²Institut für Geowissenschaften, Goethe-University Frankfurt, 60438 Frankfurt, Germany.*

13 *³LGAGE, Département de Géologie, Université Hassan-II de Casablanca, Casablanca,*
14 *Morocco.*

15 *⁴Departament de Mineralogia, Petrologia i Geologia Aplicada, Universitat de Barcelona.*
16 *08028 Barcelona, Spain.*

17 *⁵Departamento de Geodinámica, Estratigrafía y Paleontología, Universidad Complutense.*
18 *28040 Madrid, Spain.*

19 *⁶Departamento de Mineralogía y Petrología and Instituto Andaluz de Ciencias de la Tierra*
20 *(UGR, CSIC), Universidad de Granada. 18071 Granada, Spain.*

21 **Corresponding author (e-mail: rarenas@ucm.es)*

22
23
24 E-mail addresses:

25 arenas@geo.ucm.es(Ricardo Arenas, corresponding author)

26 s.sanchez@geo.ucm.es (Sonia Sánchez Martínez)

27 r.albert@geo.ucm.es (Richard Albert)
28 faouziya.haissen@gmail.com (Faouziya Haissen)
29 jfsuarez@geo.ucm.es (Javier Fernández-Suárez)
30 nurpss@gmail.com (Núria Pujol-Solà)
31 andonaeg@geo.ucm.es (Pilar Andonaegui)
32 rudiez@ucm.es (Rubén Díez Fernández)
33 japroenza@ub.edu (Joaquín A. Proenza)
34 agcasco@ugr.es (Antonio Garcia-Casco)
35 gerdes@em.uni-frankfurt.de (Axel Gerdes)

36

37

38 **Abstract**

39

40 The Variscan Orogen in Iberia and the Anti-Atlas mountains in Morocco contains a
41 set of ophiolites formed between Neoproterozoic and Devonian times, during the complex
42 evolution of the NW African-Iberian margin of Gondwana. During this time interval the margin
43 evolved from an active margin (c. 750-500 Ma, the Reguibat-Avalonian-Cadomian arc), to
44 the final collision with Laurussia in Devonian times to form Pangea. In this context, one of the
45 oldest recognized ophiolite is the Bou Azzer Ophiolite from the Anti-Atlas, dated at c. 697 Ma
46 and containing two types of mafic rocks, the youngest of which have boninitic composition.
47 To the North, in the SW Iberian Massif, the Calzadilla Ophiolite contains mafic rocks also of
48 boninitic composition dated at c. 598 Ma. Farther North, in the NW Iberian Massif, the Vila de
49 Cruces Ophiolite is formed by a thick sequence of mafic rocks with arc-tholeiitic composition
50 and minor alternations of tonalitic orthogneisses dated at c. 497 Ma. In the same region, the
51 Bazar Ophiolite has a similar age of c. 495 Ma. Also in NW Iberia there is a group of
52 ophiolites with varied lithologies and dominant mafic rocks with arc-tholeiitic composition
53 (ophiolites of Careón, Purrido and Moeche), dated at c. 395 Ma. The composition of all these
54 peri-Gondwanan ophiolites is of supra-subduction zone type showing no evidence for

55 preserved MORB-type oceanic lithosphere. Consequently, these ophiolites were generated
56 in the peri-Gondwanan realm during the opening of fore-arc or back-arc basins. Fore-arc
57 oceanic lithosphere was promptly obducted or accreted to the volcanic arc, but the oceanic
58 or transitional lithosphere generated in back-arc settings was preserved until the assembly of
59 Pangea. Based on the ages of the described ophiolites, the peri-Gondwanan realm has been
60 a domain where generation of oceanic or transitional lithosphere seems to have occurred at
61 intervals of c. 100 Ma. These regularly spaced time intervals may indicate cyclic events of
62 mantle upwelling in the peri-Gondwanan mid-ocean ridges, with associated higher
63 subduction rates at the peri-Gondwanan trenches and concomitant higher rates of partial
64 melting in the mantle wedges involved. The origin of the apparent cyclicity for mantle
65 upwelling in the peri-Gondwanan ocean ridges is unclear, but it could have been likely
66 related to episodic deep mantle convection. Cycles of more active deep mantle convection
67 can explain episodic mantle upwelling, transition from low to fast spreading type mid-ocean
68 ridges and finally the dynamic context for the episodic generation of new supra-subduction
69 zone type oceanic peri-Gondwanan lithosphere.

70

71

72 **Introduction**

73

74 The NW African-Iberian margin of Gondwana (including proto-Gondwana) was
75 characterized by a protracted evolution since Neoproterozoic times until the final assembly of
76 Pangea in Devonian and Carboniferous times. Between c. 780 Ma (Cryogenian) and c. 500
77 Ma (Late Cambrian), it represented an active margin with generation of abundant and rather
78 continuous magmatism (Fuenlabrada et al., 2010, 2020; Albert et al., 2015). Later on, since
79 Late-Cambrian to Early Ordovician times, frontal subduction and/or slab roll-back and trench
80 retreat favored extension in the upper plate lithosphere and, hence, rifting and subsequent
81 drift of peri-Gondwanan terranes. The most prominent separation was that of the Avalonian
82 terrane and the associated opening of the Rheic Ocean at its wake (Nance et al., 2010).

83 Thick sedimentary series were deposited on the Gondwanan margin between Cryogenian
84 and Ordovician times. Tectonically alternating with these series, several obducted mafic-
85 ultramafic units (ophiolites) account for the opening and closure of some minor oceanic or
86 transitional domains. The presence of these ophiolites suggests that the evolution of the
87 margin was complex and controlled by variable interactions between the subducting peri-
88 Gondwanan oceanic lithosphere, the magmatic arcs, and the mainland. During Early-Middle
89 Devonian times, dextral convergence between Gondwana and Laurussia resulted in the
90 consumption of the Rheic Ocean and continental collision that led to the final amalgamation
91 of Pangea. Two events of high-P metamorphism separated in time (at c. 400 and 370 Ma)
92 clearly indicate that this collision was complex, and contractional events alternated with
93 lithospheric extension and the opening of new ephemeral oceanic domains (Fernández-
94 Suárez et al., 2007; Abati et al., 2010; Arenas et al., 2014a; Díez Fernández et al., 2020).
95 Remnants of these oceanic domains are preserved as ophiolitic units along the Variscan
96 Orogen (Arenas and Sánchez Martínez, 2015).

97

98 The mafic-ultramafic units preserved in these ophiolites are remnants of deep
99 dynamics processes associated with the protracted evolution of the NW African-Iberian
100 margin of Gondwana. The ophiolites currently appear in the Anti-Atlas Domain of Morocco
101 and in many of the massifs that define the Variscan Orogen, notably in the Iberian Massif.
102 During the past twenty years, knowledge about these ophiolites has increased substantially,
103 including their existence, distribution, geochemical characteristics, and chronology. Dating of
104 mafic-ultramafic sequences is difficult as these lithologies contain no or scarce zircon, the
105 most amenable mineral to obtain precise U-Pb ages for the protoliths. However, the
106 chronology of the protoliths of these oceanic sequences is now well constrained. Also,
107 significant data exist that allow reconstructing parts of their obduction chronology and the
108 primary location of the oceanic or transitional domains. Dates of the ophiolitic units have
109 revealed an apparent cyclicity in the opening of oceanic or transitional domains along the
110 peri-Gondwanan realm. The origin and meaning of this cyclicity is yet unclear, but its

111 existence indicates that repetitive major-scale processes have significantly conditioned the
112 evolution of the peri-Gondwanan realm.

113

114 This work presents a review of the available U-Pb age data that support the existence
115 of cyclicity in the development of the mafic-ultramafic sequences of Morocco and the Iberian
116 Massif. The main geochemical features of the mafic rocks are also presented in order to
117 extract inferences pertaining to the tectonic setting of generation of the different oceanic or
118 transitional domains. Possible geodynamic scenarios that could have favored this cyclicity
119 are discussed, although we are still probably far from a detailed understanding of the
120 processes involved. However, the mere discovery of this cyclicity is a solid first step towards
121 some kind of understanding of the processes involved.

122

123

124 **Geological Setting**

125

126 The reconstruction of Pangea at the end of the Paleozoic (Fig. 1) shows the position
127 of the Anti-Atlas Domain in relation to the Iberian Massif. The pre-Pangean location of both
128 regions in the margin of Gondwana is difficult to reconstruct, due to both the oroclinal folding
129 and the long strike-slip shear zones that characterize the Variscan Orogen (Martínez Catalán
130 et al., 2007, 2011; Weil et al. 2013; Gutiérrez-Alonso et al., 2015) that may have probably
131 produced large displacements in the initial location of some regions. However, based on their
132 present location (Fig. 1), the original pre-Variscan distance between the Anti-Atlas and the
133 southern (non-Avalonian) part of the Iberian Massif, can be estimated at least in c. 1500-
134 2000 km. Consequently, this large spatial separation and the long time interval recorded in
135 the associated stratigraphic record, make the studied section a representative domain of the
136 large-scale dynamic evolution of the NW African-Iberian margin of Gondwana.

137

138 Located to the South of the High Atlas Mountain Range, the Anti-Atlas Domain
139 contains the northernmost outcrops of formations equivalent to those found further South in
140 the realm of the West African Craton (Michard et al., 2010; Brahimy et al., 2018; Soulimani
141 et al., 2019). Several tectonic windows or inliers show Paleoproterozoic (c. 2.2-2 Ga) to Late
142 Ediacaran formations which are overlain by thick Paleozoic series (Fig. 2). In the Bou Azzer
143 inlier, a large unit of mafic-ultramafic rocks represents the only coherent ophiolite described
144 so far in NW Africa. The c. 700 Ma Bou Azzer Ophiolite has been described as a peri-proto-
145 Gondwanan ophiolite tectonically emplaced above continental rifting series formed at c. 750-
146 700 Ma and unconformably covered by siliciclastic sedimentary rocks, the Tiddiline unit
147 (Leblanc, 1976; Ahmed et al., 2005; El Hadi et al., 2010). The ophiolite is intruded by two
148 groups of arc-related granitic rocks. A first suite of syn-kinematic diorite-tonalite plutons
149 dated at c. 653-640 Ma, followed by late-kinematic granodiorite plutons dated at c. 579-578
150 Ma (Inglis et al., 2004). The age of the syn-kinematic granitoids is also considered the
151 obduction age of the ophiolite onto the continental margin (El Hadi et al., 2010).

152

153 The Iberian Massif is characterized by the presence of large allochthonous
154 complexes which appear in the uppermost structural positions and were thrust above
155 parautochthonous and autochthonous domains during the Variscan Orogeny (Fig. 3; see
156 Arenas et al., 2016a and Díez Fernández et al., 2016 for review). Similar allochthonous
157 complexes can be found along other regions of the Variscan Orogen (Fig. 1; Ballèvre et al.,
158 2014; Martínez Catalán et al., 2020). These complexes contain a thick stack of terranes with
159 different origin and tectonothermal evolution. They include a variety of ophiolitic units that
160 appear emplaced between continental or arc-derived terranes affected by two different
161 Variscan high-P metamorphic events dated at c. 400 and 370 Ma (Arenas et al., 2014a). The
162 presence of these ophiolites has allowed the identification of more than one suture in the
163 Iberian Massif, with ages ranging between Ediacaran to Devonian.

164

165 In the SW Iberian Massif, forming part of the Ossa-Morena Complex, the c. 600 Ma
166 Calzadilla Ophiolite occurs as tectonic slices imbricated with Ediacaran siliciclastic rocks of
167 the so called Serie Negra Group (Fig.3). Both the ophiolite and the surrounding
168 metasedimentary series have been interpreted as the remnants of an Ediacaran fore-arc
169 basin opened in the most external section of the active margin of Gondwana (Arenas et al.,
170 2018). The imbrication and final obduction of the ophiolite above the continental margin
171 probably occurred in the Ediacaran – Early Cambrian boundary (Arenas et al., 2018; Díez
172 Fernández et al., 2019).

173

174 In the NW of the Iberian Massif, the ophiolites considered in this work form part of the
175 Órdenes and Cabo Ortegal allochthonous complexes. Equivalent ophiolites are present in
176 the allochthonous complexes located more to the SE in the Portuguese region of Trás-os-
177 Montes (Fig. 3; Martínez Catalán et al., 2020). Two ophiolitic units dated at c. 500 Ma have
178 been described in the large Órdenes Complex of Galicia (Fig. 3). In the western part of this
179 complex, the Bazar Ophiolite is defined by a mafic-ultramafic sequence characterized by a
180 large geochemical variation. This unit was described as a ridge-derived ophiolite accreted
181 below a dissected peri-Gondwanan volcanic arc in Early Ordovician times (Sánchez Martínez
182 et al., 2012). Low-P granulite facies metamorphism recognized in the mafic rocks was dated
183 at c. 475 Ma and is considered an indication of ridge-subduction. In the eastern part of the
184 Órdenes Complex, the c. 500 Ma Vila de Cruces Ophiolite consists of a thick imbricate unit of
185 greenschist facies mafic rocks, schists and phyllites, with a few levels of orthogneisses and
186 serpentinites in the upper part of the unit. This Cambrian ophiolite was interpreted as a
187 typical back-arc ophiolite based on its characteristic geochemical pattern (Arenas et al.,
188 2007; Arenas and Sánchez Martínez, 2015). However, unlike the ophiolites described before,
189 no evidence of a pre-Variscan obduction was found in the Vila de Cruces ophiolite. The
190 tectonic fabrics dated in this ophiolite (c. 363-367 Ma, $^{40}\text{Ar}/^{39}\text{Ar}$ dating; Dallmeyer et al., 1997)
191 indicate the accretion to an orogenic crust and the final subsequent obduction onto a

192 continental margin during the main Variscan orogenic events. These data seem to indicate
193 that large back-arc basins existed for a long period in the peri-Gondwanan realm.

194

195 Three different Middle Devonian ophiolites (c. 400 Ma) are mentioned in this work: the
196 Careón Ophiolite, in the eastern section of the Órdenes Complex, and the Purrido and
197 Moeche ophiolites, in the western and eastern parts of the Cabo Ortegal Complex,
198 respectively (Fig. 3). The Careón Ophiolite was the first ophiolite dated in the Iberian Massif,
199 and probably also the first ophiolite presented as a supra-subduction zone type in the
200 Variscan Orogen (Díaz García et al., 1999; Sánchez Martínez et al., 2007). Similar ages and
201 classification emerged successively for the Purrido and Moeche ophiolites (Arenas and
202 Sánchez Martínez, 2015). The protoliths of these ophiolites were generated in between the
203 two high-P metamorphic events characteristic of the Variscan Orogen. Considering this
204 chronology and the presence of very old zircon remnants in these ophiolites (Sánchez
205 Martínez et al., 2011), they were probably formed during the opening of an ephemeral
206 synorogenic basin during the main events of the Pangea assembly, either of pull-apart
207 (Arenas et al., 2014a) or supra-subduction zone type (Díez Fernández et al., 2020). This
208 buoyant oceanic lithosphere was likely obducted soon after its generation, as suggested by
209 $^{40}\text{Ar}/^{39}\text{Ar}$ ages of the amphibolite facies foliation of the Careón and Purrido ophiolites ranging
210 between c. 391 and 377 Ma (Peucat et al., 1990; Dallmeyer et al., 1997).

211

212 It is also relevant to note that a younger ophiolite (not considered in this work) has
213 been described in the Iberian Massif, the Beja-Acebuches Ophiolite, dated at c. 340-332 Ma
214 (Azor et al., 2008). This ophiolite is located at the northern boundary of the South Portuguese
215 Zone (Fig. 3). This boundary is considered the true main suture developed during the final
216 assembly of Pangea, because it separates Gondwana from the southern margin of Laurussia
217 (Figs. 1 and 3). Consequently, it represents the original location of the Rheic Ocean suture,
218 but this region was strongly reworked during the Variscan deformation which caused the

219 opening of a new syn-orogenic basin and the final obduction of a Carboniferous ophiolite
220 (Díez Fernández et al., 2016).

221

222

223 **Ophiolite sequences**

224

225 Representative columns that show the architecture of the ophiolites described in this
226 work can be seen in Figure 4. With the exception of the Bou Azzer Ophiolite, the mafic-
227 ultramafic sequences considered in the peri-Gondwanan realm do not show typical mid-
228 ocean ridge architectures. On the contrary, they appear as alternations of ultramafic units
229 with other sections formed by gabbroic rocks and/or their metamorphic products, either
230 amphibolites, greenschists or rare granulites. In these plutonic sections, tonalitic
231 compositions are very rare, although they do exist. Typical mid-ocean ridge sections
232 characterized by the presence of volcanic rocks and a sheeted dyke complex are in general
233 absent. The general architecture of these ophiolites strongly suggests that they were formed
234 in a tectonic setting different to that of mid-ocean ridges, probably in supra–subduction zone
235 regions.

236

237 The architecture of the c. 700 Ma Bou Azzer Ophiolite described in Figure 4 is based
238 on the map and cross sections presented by El Hadi et al. (2010). It is composed of a single
239 c. 5-6 km thick ophiolite column lacking tectonic imbrications. However, the existence of
240 internal imbrication cannot be ruled out because the ophiolite is unusually thick. In the
241 ophiolite, a lower unit of ultramafic rocks, dominated by serpentinites, is followed by a
242 plutonic unit of variably deformed gabbros and layered gabbros metamorphosed under
243 amphibolite facies conditions. An upper section of undifferentiated volcanic rocks and dykes
244 has been described in this ophiolite, immediately below the basal unconformity of the
245 Tiddiline siliciclastic formation. Moreover, a set of scarce doleritic dykes intrude the peridotitic
246 and gabbroic units, indicating a second magmatic event.

247

248 The column of the c. 600 Ma Calzadilla Ophiolite is characterized by a c. 1 km thick
249 lower mafic-ultramafic unit and some upper imbrications of serpentinites and Ediacaran
250 metagreywackes of the Serie Negra Group (Fig. 4; Arenas et al. 2018). The c. 800 m thick
251 basal ultramafic section is composed of harzburgites, dunites, amphibole-bearing peridotites
252 and some pyroxenites, which show moderate serpentinization. Distributed in the host
253 dunites, some sectors contain abundant high-Al podiform chromitites (Merinero et al., 2013),
254 typical of the mantle-crust transition zone (Moho discontinuity). These rocks may therefore
255 be related to the contact between the ultramafic unit and the c. 200 m thick plutonic unit. The
256 latter is exclusively formed by medium-coarse metagabbros metamorphosed under
257 amphibolite facies conditions.

258

259 The c. 500 Ma Bazar Ophiolite is composed of two main slices with a total thickness
260 of c. 5 km (Fig. 4; Sánchez Martínez et al., 2012). However, taking into account that the
261 thickness of this ophiolite is significant, internal imbrications cannot be discarded, especially
262 in the thicker mafic unit. The upper slice is the thickest and includes a lower section of
263 moderately serpentinized ultramafic rocks which appear in complex alternations with a large
264 diversity of gabbros, leucogabbros and tonalitic stocks. These plutonic rocks indicate high
265 intrusive activity over the upper section of the lithospheric mantle. The mafic section is
266 formed by gabbros, melagabbros, high-T amphibolites and common amphibolites. In the less
267 deformed sectors, lens-shaped bodies of low-P mafic granulites account for an initial high-T
268 metamorphic event affecting this unit.

269

270 The c. 500 Ma-aged Vila de Cruces Ophiolite consists of an imbrication of several
271 slices that include mafic rocks, schists and phyllites (Arenas et al., 2007). The mafic rocks
272 consist of highly sheared greenschists that, in the upper part of the unit, include some
273 alternations of thin tonalitic orthogneisses and serpentinites. Distributed within the

274 greenschists, a few remnants of low to moderately sheared metagabbros can also be locally
275 observed.

276

277 The Careón Ophiolite is the most representative unit for the c 400 Ma ophiolites, and
278 also the one that was first dated and described in some detail (Díaz García et al., 1999;
279 Sánchez Martínez et al., 2007). It consists of three slices that apparently repeat an oceanic
280 mantle-crust transition zone. This paleo Moho region locally shows the development of
281 metamorphic soles with evidence of high-T metamorphism. The larger intermediate slice, the
282 Careón slice (Fig. 4), reaches a thickness of c. 1000 m, being constituted by a lower
283 ultramafic section and an upper plutonic section, both with a similar thickness. The ultramafic
284 section contains serpentized peridotites, intruded by frequent stocks of gabbros, pegmatoid
285 gabbros and doleritic dykes. The plutonic section is constituted by gabbros, layered gabbros
286 and pegmatoid gabbros, which also appear intruded by numerous doleritic dykes (Díaz
287 García et al., 1999). Included also in this group, the Purrido and Moeche ophiolites comprise
288 thinner sequences of common metagabbroic amphibolites and sheared greenschists with
289 some alternations of phyllites and minor serpentinites, respectively (Arenas and Sánchez
290 Martínez, 2015).

291

292

293 **Zircon U-Pb ages and Hf isotope composition**

294

295 U-Pb ages and isotopic Hf data of 258 zircons from the investigated ophiolites are
296 plotted in the U-Pb age (Ma) versus $\epsilon\text{Hf}(t)$ diagram of Figure 5. In this plot, the $^{206}\text{Pb}/^{238}\text{U}$
297 ages (of concordant analyses) were preferred for representation. This data collection
298 contains all the published geochronological and isotopic information available for the
299 ophiolites considered in this work. The data presented in Figure 5 clearly show the four age
300 groups separated by c. 100 Ma gaps. The protoliths of these peri-Gondwanan ophiolites

301 were formed in the Neoproterozoic and the Paleozoic in four main events of generation of
302 oceanic or transitional lithosphere, at c. 700, 600, 500 and 400 Ma.

303

304 Data from the Neoproterozoic c. 700 Ma-aged Bou Azzer Ophiolite are taken from the
305 U-Pb data (SHRIMP) of a gabbro dated at 697 ± 6 Ma (El Hadi et al., 2010). However,
306 isotopic Hf data were not obtained for zircon in this ophiolite and therefore it is not possible to
307 make deductions about the associated isotopic sources. Just in order to plot the U-Pb ages
308 in this diagram and compare the number of analyses, we have assigned arbitrarily depleted
309 mantle $\epsilon\text{Hf}(t)$ values (Fig. 5). In the case of the c. 600 Ma Calzadilla Ophiolite, U-Pb ages
310 (SHRIMP) and isotopic Hf (LA-ICP-MS) were obtained in a metagabbro dated at c. 598 ± 10
311 Ma (Arenas et al., 2018). $\epsilon\text{Hf}(t)$ values are in general higher than 10 and indicate a juvenile
312 origin for the gabbroic protoliths (Fig. 5). However, scarce zircon data with $\epsilon\text{Hf}(t) < 8$ may
313 suggest limited isotopic mixing and interaction with older isotopic sources, which is in
314 agreement with a peri-continental or peri-arc setting for this ophiolite.

315

316 Considered as a whole, the U-Pb zircon ages (LA-ICP-MS) of the Cambrian Bazar
317 and Vila de Cruces ophiolites show an average age at c. 500 Ma (Fig. 5). In the Bazar
318 Ophiolite, these ages correspond to an ophiolitic metagabbro dated at 495 ± 2 Ma (Sánchez
319 Martínez et al., 2012). Data for the Vila de Cruces Ophiolite has been obtained in a
320 metagabbro and three tonalitic orthogneisses (Sánchez Martínez et al., 2020, this volume).
321 All $\epsilon\text{Hf}(t)$ data plot around the depleted mantle evolution trend, suggesting juvenile or near-
322 juvenile isotopic sources for the protoliths, even in the case of the tonalitic rocks (Fig. 5). One
323 of this tonalitic orthogneisses yielded the first U-Pb age for this ophiolite at c. 497 ± 4 Ma
324 (TIMS; Arenas et al., 2007).

325

326 The available age data for the Devonian ophiolites are based on the U-Pb zircon
327 dating of a leucocratic metagabbro of the Careón Unit (395 ± 2 Ma, TIMS; Díaz García et al.,
328 1999), two metagabbroic amphibolites of the Purrido Unit (395 ± 2 Ma, SHRIMP; Sánchez

329 Martínez et al., 2011) and a mylonitic greenschist of the Moeche Unit (400 ± 3 Ma, LA-ICP-
330 MS; Arenas et al., 2014b). The isotopic Hf zircon data in these ophiolites (Purrido and
331 Moeche ophiolites; LA-ICP-MS) show two different populations, with contrasted $\epsilon\text{Hf}(t)$ values
332 (Fig. 5). A first group of zircons with rather high $\epsilon\text{Hf}(t)$ values reveals the presence of juvenile
333 magmas in the origin of these Devonian ophiolites. However, another group of zircons show
334 negative $\epsilon\text{Hf}(t)$ values, which indicate the participation of older isotopic sources. Taken
335 together, the isotopic Hf data define a marked mixing line that should have been active
336 during the generation and emplacement of the original mafic magmas (Fig. 5). This evolution
337 can only be generated during the interaction of the mafic protoliths with a region
338 characterized by the presence of old isotopic sources, i.e. a continental domain or a volcanic
339 arc rooted by an old continental basement.

340

341

342 **Immobile trace element geochemistry and geodynamic setting**

343

344 The geochemistry of immobile elements has proven to be the most efficient tool to
345 decipher the dynamic setting of ophiolite generation (Pearce and Cann, 1971; Pearce, 1996,
346 2014). The origin of the described ophiolites has been investigated using a database of 117
347 chemical analyses of immobile trace elements. The database is sourced from published
348 information, with the exception of the analyses of the Bou Azzer Ophiolite, which were
349 obtained for this study. The database includes: 12 analyses from the Bou Azzer Ophiolite,
350 including gabbros (6 samples) and doleritic dykes (6 samples); 10 analyses of gabbros from
351 the Calzadilla Ophiolite (Arenas et al., 2018); 16 analyses from the Bazar Ophiolite (Sánchez
352 Martínez et al., 2012), including metagabbros (5 samples), amphibolites (7 samples) and
353 mafic granulites (4 samples); 16 analyses from the Vila de Cruces Ophiolite (Arenas et al.,
354 2007), including metagabbros (4 samples) and greenschists (12 samples); 32 analyses from
355 the Careón Ophiolite (Sánchez Martínez et al., 2007), including gabbros (15 samples),
356 doleritic dykes (9 samples) and amphibolites (8 samples); 18 amphibolites from the Purrido

357 Ophiolite (Sánchez Martínez et al., 2011) and 13 greenschists from the Moeche Ophiolite
358 (Arenas et al., 2014b).

359

360 The Nb/Yb versus Th/Yb diagram (Fig. 6) separates the field of mafic magmas
361 generated in non-subduction settings (N-MORB-OIB array), from the domain where the
362 magmas derived from supra-subduction zone settings. These regions are characterized by
363 mantle modification by subduction-derived fluids and the composition of melts is displaced
364 towards higher Th/Yb ratios (Pearce, 2014). Magmas modified by assimilation of continental
365 crust form diagonal lines in which both Th and Nb are modified. These lines define trends
366 that extend from the N-MORB-OIB array into the island-arc or continental-arc fields. These
367 magmas can also show a characteristic high dispersion in this diagram. This geochemical
368 pattern is considered a diagnostic feature for back-arc basin settings and has also been
369 described in ridge subduction and, more rarely, in continental margin settings (Pearce,
370 2014). The distribution of the peri-Gondwanan ophiolitic basaltic rocks in this diagram clearly
371 shows that most of them, if not all, pertain to supra-subduction type ophiolites. These
372 ophiolites are hence derived from oceanic or transitional lithosphere formed above peri-
373 Gondwanan subduction zones, after partial melting of mantle wedges modified by the ascent
374 fluids generated during dehydration of the subducted slab. The mafic rocks of the Bou Azzer,
375 Calzadilla and Vila de Cruces ophiolites plot far from the MORB-OIB array, in regions typical
376 of magmas formed in supra-subduction zone settings (SSZ), near volcanic arcs (Fig. 6). The
377 geochemistry of the Bazar Ophiolite is much more complex because it is characterized by
378 the presence of different magma types and larger dispersion (Fig. 6). This pattern has been
379 described in magmas formed in settings characterized by ridge subduction (Pearce, 2014).
380 This was the dynamic setting initially suggested for the Bazar Ophiolite, based on the
381 accretion of this ophiolite immediately following the generation of the mafic protoliths, with
382 the development of a prograde low to intermediate-P granulite facies metamorphism
383 (Sánchez Martínez et al., 2012). The composition of the Devonian Careón, Purrido and
384 Moeche ophiolites is also indicative of their generation in a supra-subduction zone setting.

385 Taking together, these three coeval ophiolites show a projection characterized by a large
386 dispersion (Fig. 6). Moreover, the plotted analyses define diagonal lines passing from the
387 MORB-OIB array to the SSZ field, which is compatible with assimilation of continental
388 material during the ascent of the mafic magmas in a supra-subduction zone setting (Pearce,
389 2014).

390

391 The Ti versus V diagram (Fig. 7) can be used to refine the origin of mafic magmas
392 previously characterized as SSZ types in the Nb/Yb vs. Th/Yb diagram (Shervais, 1982;
393 Pearce, 2014). Excluding the unusual composition of the mafic rocks of the Bazar Ophiolite,
394 most of the data plot in the field of basalts generated in slab-distal regions, either in back-arc
395 basin or fore-arc basin settings, although the rocks of the Vila de Cruces Ophiolite are
396 divided into slab-proximal and slab-distal fields (Fig. 7). Additionally, the rocks of the
397 Ediacaran Calzadilla Ophiolite appear as typical boninites, according to the previous
398 classification of the mafic rocks of this ophiolite (Arenas et al., 2018). In the case of the older
399 Bou Azzer ophiolite, the group of mafic rocks that correspond to boninite compositions (Fig.
400 7) includes the younger doleritic dykes that intrude all levels of the ophiolite, including the
401 harzburgitic mantle. Boninitic magmas are considered to be generated from ultra-depleted
402 harzburgitic sources, which result from previous melting events that removed most of the
403 incompatible elements (Dobson et al., 2006). Repetitive melting affects a stable mantle
404 wedge, i.e. a mantle section not affected by significant convection. The Bou Azzer Ophiolite
405 shows the characteristics of a subduction-initiation ophiolite, where magmas in this diagram
406 evolve from MORB-like when subduction begins, to more boninite-like as subduction
407 proceeds (Pearce, 2014).

408

409

410 **Discussion**

411

412 *SSZ ophiolite: the common ophiolitic type in the peri-Gondwanan realm*

413

414 Taking into account the distribution of the investigated ophiolites in Iberia and the
415 Anti-Atlas domain, their lithological constitution, chronology and geochemistry, it can be
416 concluded that the SSZ ophiolite type represents the most characteristic ophiolitic type in the
417 NW African-Iberian peri-Gondwanan realm. Consequently, the NW African-Iberian margin of
418 Gondwana was a large region where new oceanic or transitional lithosphere was generated
419 in successive events in SSZ contexts (Fig. 8). This conclusion is in good agreement with
420 previous studies pointing out that the NW African-Iberian margin of Gondwana was an active
421 margin at least between Cryogenian and Cambrian times, i.e. a large region where
422 subduction was active during a long time (Pereira et al., 2012; Linnemann et al., 2014; Albert
423 et al., 2015; Fuenlabrada et al., 2016, 2020; Rojo-Pérez et al., 2019). There is not clear
424 evidence for typical MORB compositions in the mafic rocks of the considered peri-
425 Gondwanan ophiolites. The cold and dense lithosphere of the peri-Gondwanan oceans was
426 continuously subducted, without any detected MORB remains in the investigated ophiolites.
427 Conversely, the newly created SSZ oceanic lithospheres were characterized by buoyant
428 nature in relation to accretionary processes. In the cases where the new oceanic lithosphere
429 was generated in fore-arc realms, it was rapidly transferred to the peri-Gondwanan volcanic-
430 arc system. On the contrary, the oceanic lithosphere generated in back-arc basins was
431 preserved with little change and progressively covered by thick sedimentary series. These
432 back-arc domains were finally deformed and obducted during the assembly of Pangea.

433

434 It has been proposed that the obduction of the Bou Azzer Ophiolite took place in the
435 context of a basin located in between the proto-Gondwanan mainland and a volcanic arc at
436 c. 579-578 Ma (El Hadi et al., 2010). The generation in Neoproterozoic times (at c. 700 Ma)
437 of the oceanic lithosphere represented by this ophiolite, occurred near the most external
438 section of Reguibat, in the NE margin of the West African Craton. This location and the
439 generation of boninitic magmas following the extrusion of common SSZ basalts, suggest a
440 typical external fore-arc domain as the most probable dynamic setting for the formation of the

441 Bou Azzer Ophiolite (Fig. 8). This ophiolite was likely generated above the peri-proto-
442 Gondwanan trench where the lithosphere of the Pharusian Ocean was subducted (Fig. 8).
443 This ophiolite was likely obducted onto a section of the West African Craton covered by
444 rifting-related sedimentary series (El Hadi et al., 2010). A similar fore-arc generation has
445 been proposed for the Calzadilla Ophiolite, where the composition of the gabbroic rocks is
446 also boninitic (Fig. 8). This ophiolite was probably obducted onto the continental margin at c.
447 540 Ma, according to U-Pb zircon age and detailed structural data that allow reconstructing
448 the tectonothermal evolution underwent by this ophiolite (Arenas et al., 2018; Díez
449 Fernández et al., 2019). In the case of the c. 500 Ma ophiolites, the scenario seems more
450 varied. The Bazar Ophiolite was probably also generated in a fore-arc setting, according to
451 its geochemical characteristics and prompt accretion at c. 475 Ma (Sánchez Martínez et al.,
452 2012). However, the Vila de Cruces Ophiolite is characterized by a thick sedimentary cover
453 and was not apparently affected by deformation and metamorphism until the onset of the
454 Variscan deformation. This suggests that the protoliths of this ophiolite were preserved in a
455 long-lasting stable back-arc basin (Fig. 8).

456

457 The generation of the Devonian ophiolites appears to have been much more
458 complex. The protoliths of these ophiolites were generated in between the two high-P
459 Variscan metamorphic events dated at c. 400 and 370 Ma (Arenas et al., 2014a). Their
460 chronology (c. 400 Ma) hence implies that they were generated in relation to some type of
461 basin opened in the middle of the already assembled Pangea (Fig. 9). Pull-apart or supra-
462 subduction zone models have been considered for the opening of this basin (Arenas et al.,
463 2014a; Díez Fernández et al., 2020). However, our current knowledge may not be detailed
464 enough yet to decipher the tectonic context where this basin was generated. Different
465 possibilities for related subduction and/or strike-slip tectonics exist. Besides, the generation
466 of this SSZ oceanic crust in the middle of Pangea in Devonian times, implies participation of
467 a mantle section that was previously hydrated during long subduction. This mantle section

468 was apparently located in the distal margin of Gondwana that was affected by collision with
469 Laurussia (Arenas et al., 2016; Díez Fernández et al., 2016).

470

471

472 *100 Ma cycles of mantle upwelling*

473

474 The NW African-Iberian margin of Gondwana faced an ocean for a long time,
475 probably before the amalgamation of Rodinia (Torsvik, 2003). During most of this period,
476 peri-Gondwanan subduction zones were active, favoring continuous hydration and episodic
477 partial melting of the related mantle wedges. This margin was also characterized by a
478 dynamic setting where frequent generation of new supra-subduction oceanic or transitional
479 oceanic crust occurred (Fig. 8). According to the chronology of the peri-Gondwanan
480 ophiolites, new oceanic lithospheres were generated in cycles separated by c. 100 Ma. The
481 reason for this cyclicity is unclear, but in any case the peri-Gondwanan ophiolites clearly
482 highlight these cycles and are therefore a key starting point in furthering our understanding of
483 the scenarios involved.

484

485 First, it can be proposed that each new event of generation of oceanic lithosphere
486 was triggered by increasing rates of partial melting in the mantle wedge above the
487 subduction zone. These episodic events occurred in the context of the large peri-Gondwanan
488 arc-system, giving rise to more or less ephemeral fore-arc or back-arc basins with SSZ type
489 oceanic or transitional lithosphere. The activation of higher rates of mantle partial melting can
490 be related to accelerate fluid percolation in the mantle wedge, which in turn indicates
491 increasing subduction rates. Variable subduction rates can be caused by changes in the
492 intensity of mantle upwelling in the central ridges of the peri-Gondwanan oceans. Since we
493 have found no trace of MORB-type lithosphere in the peri-Gondwanan ophiolites, it can be
494 concluded that the whole peri-Gondwanan oceans were entirely consumed by subduction.
495 However, these were probably large oceans with central ridges active during a long period,

496 according to the activity of the peri-Gondwanan volcanic-arc systems. The origin of the
497 revealed cyclicity of mantle upwelling in the peri-Gondwanan oceans ridges can be related to
498 deep episodic mantle convection (Richter, 1973; Coltice et al., 2019). Cycles of more active
499 deep mantle convection can explain episodic mantle upwelling, transition from low to fast
500 type mid-ocean ridges, higher subduction rates, and finally, the dynamic context for the
501 episodic generation of new supra-subduction zone type oceanic or transitional peri-
502 Gondwanan lithosphere in regions undergoing extension. The causes for these evenly
503 spaced c. 100 Ma fast-ridge cycles may be connected with secular long term heat exchange
504 between the outer core and the lower mantle. Different long-term and short-term cycles of
505 mantle activity since Paleoproterozoic times have been recently revealed on Earth (Li et al.,
506 2019; Mitchell et al., in press). The cyclicity discovered in the generation of new oceanic
507 crust in the peri-Gondwanan realm, provides first order evidence to further understanding
508 mantle cycles since Neoproterozoic times. In this context, the peri-Gondwanan ophiolites
509 appear as key units that can unexpectedly provide valuable information on this question.

510

511

512 **Acknowledgements**

513

514 Insightful revision of the manuscript by Francisco Pereira and Robin Shail is kindly
515 acknowledged. Excellent edition of the manuscript by Brendan Murphy is also appreciated.
516 Financial support has been provided by the Spanish projects CGL2016-76438-P and
517 CGL2015-65824 (Ministerio de Economía, Industria y Competitividad) and a FPU grant to
518 N.P.S. (Ministerio de Educación). The help extended by MANAGEM mining holding is
519 gratefully acknowledged.

520

521

522 **References**

523

524 Abati, J., Gerdes, A., Fernández-Suárez, J., Arenas, R., Whitehouse, M.J. & Díez
525 Fernández, R. 2010. Magmatism and early-Variscan continental subduction in the
526 northern Gondwana margin recorded in zircons from the basal units of Galicia, NW Spain.
527 *Geological Society of America Bulletin*, **122**, 219-235.

528

529 Ahmed, A.H., Arai, S., Abdel-Aziz, Y.M. & Rahimi, A. 2005. Spinel composition as a
530 petrogenetic indicator of the mantle section in the Neoproterozoic Bou Azzer ophiolite,
531 Anti-Atlas, Morocco. *Precambrian Research*, **138**, 225-234.

532

533 Albert, R., Arenas, R., Gerdes, A., Sánchez Martínez, S. & Marko, L. 2015. Provenance of the
534 HP-HT subducted margin in the Variscan belt (Cabo Ortegal Complex, NW Iberian
535 Massif). *Journal of Metamorphic Geology*, **33**, 959-979.

536

537 Arenas, R., Martínez Catalán, J.R., Sánchez Martínez, S., Fernández-Suárez, J.,
538 Andonaegui, P., Pearce, J.A. & Corfu, F. 2007. The Vila de Cruces Ophiolite: A remnant
539 of the early Rheic Ocean in the Variscan suture of Galicia (NW Iberian Massif). *Journal of*
540 *Geology*, **115**, 129-148.

541

542 Arenas, R., Díez Fernández, R., Sánchez Martínez, S., Gerdes, A., Fernández-Suárez, J. &
543 Albert, R. 2014a. Two-stage collision: Exploring the birth of Pangea in the Variscan
544 terranes. *Gondwana Research*, **25**, 756-763.

545

546 Arenas, R., Sánchez Martínez, S., Gerdes, A., Albert, R., Díez Fernández, R. & Andonaegui,
547 P. 2014b. Re-interpreting the Devonian ophiolites involved in the Variscan suture: U-Pb
548 and Lu-Hf zircon data of the Moeche Ophiolite (Cabo Ortegal Complex, NW Iberia).
549 *International Journal of Earth Sciences*, **103**, 1385-1402.

550

551 Arenas, R. & Sánchez Martínez, S. 2015. Variscan ophiolites in NW Iberia: Tracking lost
552 Paleozoic oceans and the assembly of Pangea. *Episodes*, **38**, 315-333.

553

554 Arenas, R., Sánchez Martínez, S., Díez Fernández, R., Gerdes, A., Abati, J., Fernández-
555 Suárez, J., Andonaegui, P., González Cuadra, P., López Carmona, A., Albert, R.,
556 Fuenlabrada, J.M. & Rubio Pascual, F.J. 2016a. Allochthonous terranes involved in the
557 Variscan suture of NW Iberia: A review of their origin and tectonothermal evolution. *Earth-
558 Science Reviews*, **161**, 140-178.

559

560 Arenas, R., Díez Fernández, R., Rubio Pascual, F.J., Sánchez Martínez, S., Martín Parra,
561 L.M., Matas, J., González del Tánago, J., Jiménez-Díaz, A., Fuenlabrada, J.M.,
562 Andonaegui, P. & García-Casco, A. 2016b. The Galicia-Ossa-Morena Zone: Proposal for
563 a new zone of the Iberian Massif. Variscan implications. *Tectonophysics*, **681**, 135-143.

564

565 Arenas, R., Fernández-Suárez, J., Montero, P., Díez Fernández, R., Andonaegui, P.,
566 Sánchez Martínez, S., Albert, R., Fuenlabrada, J.M., Matas, J., Martín Parra, L.M., Rubio
567 Pascual, F.J., Jiménez-Díaz, A. & Pereira, M.F. 2018. The Calzadilla Ophiolite (SW Iberia)
568 and the Ediacaran fore-arc evolution of the African margin of Gondwana. *Gondwana
569 Research*, **58**, 71-86.

570

571 Azor, A., Rubatto, D., Simancas, J.F., González Lodeiro, F., Martínez Poyatos, D., Martín
572 Parra, L.M. & Matas, J. 2008. Rheic Ocean ophiolitic remnants in southern Iberia
573 questioned by SHRIMP U-Pb zircon ages on the Beja-Acebuches amphibolites.
574 *Tectonics*, **27**, TC5006.

575

576 Ballèvre, M., Martínez Catalán, J.R., López-Carmona, A., Pitra, P., Abati, J., Díez
577 Fernández, R., Ducassou, C., Arenas, R., Bosse, V., Castiñeiras, P., Fernández-Suárez,
578 J., Gómez Barreiro, J., Paquette, J.L., Peucat, J.J., Pujol, M., Ruffet, G. & Sánchez

579 Martínez, S. 2014. Correlation of the nappe stack in the Ibero-Armorican arc across the
580 Bay of Biscay: a joint French–Spanish project. *In*: Schulmann, K., Martínez Catalán, J.R.,
581 Lardeaux, J.M., Janoušek, V., Oggiano, G., (Eds) *The Variscan orogeny: extent,*
582 *timescale and the formation of the European crust. Geological Society, London, Special*
583 *Publications*, **405**, 77–113.

584

585 Brahimi, S., Liégeois, J.P., Ghienne, J.F., Munsch, M. & Bourmatte, A. 2018. The Tuareg
586 shield terranes revisited and extended towards the northern Gondwana margin: Magnetic
587 and gravimetric constraints. *Earth-Science Reviews*, **185**, 572-599.

588

589 Coltice, N., Laurent, H., Faccenna, C. & Maëlis, A. 2019. What drives tectonic plates?
590 *Science Advances*, **5**, eaax4295.

591

592 Dallmeyer, R.D., Martínez Catalán, J.R., Arenas, R., Gil Ibarguchi, J.I., Gutiérrez Alonso, G.,
593 Farias, P., Aller, J. & Bastida, F. 1997. Diachronous Variscan tectonothermal activity in
594 the NW Iberian Massif: evidence from $^{40}\text{Ar}/^{39}\text{Ar}$ dating of regional fabrics. *Tectonophysics*,
595 **277**, 307-337.

596

597 Díaz García, F., Arenas, R., Martínez Catalán, J.R., González del Tánago, J. & Dunning,
598 G.R. 1999. Tectonic evolution of the Careón Ophiolite (northwest Spain): a remnant of
599 oceanic lithosphere in the Variscan Belt. *Journal of Geology*, **107**, 587-605.

600

601 Díez Fernández, R. & Arenas, R. 2015. The Late Devonian Variscan suture of the Iberian
602 Massif: A correlation of high-pressure belts in NW and SW Iberia. *Tectonophysics*, **654**,
603 96-100.

604

605 Díez Fernández, R., Arenas, R., Pereira, M.F., Sánchez-Martínez, S., Albert, R., Martín
606 Parra, L.M., Rubio Pascual, F.J. & Matas, J. 2016. Tectonic evolution of Variscan Iberia:
607 Gondwana-Laurussia collision revisited. *Earth-Science Reviews*, **162**, 269-292.
608

609 Díez Fernández, R., Jiménez-Díaz, A., Arenas, R., Pereira, M.F. & Fernández-Suárez, J.
610 2019. Ediacaran obduction of a fore-arc ophiolite in SW Iberia: A turning point in the
611 evolving geodynamic setting of peri-Gondwana. *Tectonics*, **38**, 95-119.
612

613 Díez Fernández, R., Arenas, R., Sánchez Martínez, S., Novo Fernández, I. & Albert, R.
614 2020. Single subduction zone for the generation of Devonian ophiolites and high-P
615 metamorphic belts of the Variscan orogen (NW iberia). *Terra Nova*. In press.
616

617 Dobson, P.F., Blank, J.G., Maruyama, S. & Liou, J.G. 2006. Petrology and geochemistry of
618 boninite-series volcanic rocks, Chichi-Jima, Bonin Islands, Japan. *International Geology*
619 *Review*, **48**, 669-701.
620

621 El Hadi, H., Simancas, J.F., Martínez Poyatos, D., Azor, A., Tahiri, A., Montero, P., Fanning,
622 C.M., Bea, F. & González-Lodeiro, F. 2010. Structural and geochronological constraints
623 on the evolution of the Bou Azzer Neoproterozoic ophiolite (Anti-Atlas, Morocco).
624 *Precambrian Research*, **182**, 1-14.
625

626 Fernández-Suárez, J., Arenas, R., Abati, J., Martínez Catalán, J.R. & Whitehouse, M.J.,
627 Jeffries, T.E. 2007. U-Pb chronometry of polymetamorphic high-pressure granulites: An
628 example from the allochthonous terranes of the NW Iberian Variscan belt. *In*: Hatcher,
629 R.D. Jr., Carlson, M.P., McBride, J.H. and Martínez Catalán, J.R. (Eds.) *4-D Framework*
630 *of Continental Crust. Geological Society of America Memoir*, **200**, 469-488.
631

632 Fuenlabrada, J.M., Arenas, R., Sánchez Martínez, S., Díaz García, F. & Castiñeiras, P.
633 2010. A peri-Gondwana arc in NW Iberia. I: Isotopic and geochemical constraints on the
634 origin of the arc - A sedimentary approach. *Gondwana Research*, **17**, 338-351.

635

636 Fuenlabrada, J.M., Pieren, A.P., Díez Fernández, R., Sánchez Martínez, S. & Arenas, R.
637 2016. Geochemistry of the Ediacaran-Early Cambrian transition in Central Iberia: Tectonic
638 setting and isotopic sources. *Tectonophysics*, **681**, 15-30.

639

640 Fuenlabrada, J.M., Arenas, R., Sánchez Martínez, S., Díez Fernández, R., Pieren, A.P.,
641 Pereira, M.F., Chichorro, M. & Silva, J.B. 2020. Geochemical and isotopic (Sm-Nd)
642 provenance of Ediacaran-Cambrian metasedimentary series from the Iberian Massif.
643 Paleoreconstruction of the North Gondwana margin. *Earth-Science Reviews*, **201**. In
644 press.

645

646 Gutiérrez-Alonso, G., Collins, A.S., Fernández-Suárez, J., Pastor-Galán, D., González-
647 Clavijo, E., Jourdan, F., Weil, A.B. & Johnston, S.T. 2015. Dating of lithospheric buckling:
648 Ar-40/Ar-39 ages of syn-oroclinal strike-slip shear zones in northwestern Iberia.
649 *Tectonophysics*, **643**, 44-54.

650

651 Inglis, J.D., MacLean, J.S., Samson, S.D., D' Lemos, R.S., Admou, H. & Hefferan, K. 2004. A
652 precise U-Pb zircon age for the Bleida granodiorite, Anti-Atlas, Morocco: implications for
653 the timing of deformation and terrane assembly in the eastern Anti-Atlas Mountains.
654 *Journal of Geology*, **113**, 439-450.

655

656 Leblanc, M. 1976. Proterozoic oceanic crust at Bou Azzer. *Nature*, **261**, 34-35.

657

658 Li, Z.X., Mitchell, R.N., Spencer, C.J., Ernst, R., Pisarevsky, S., Kirscher, U. & Murphy, J.B.
659 2019. Decoding Earth's rhythms: Modulation of supercontinent cycles by longer
660 superocean episodes. *Precambrian Research*, **323**, 1-5.
661

662 Linnemann, U., Gerdes, A., Hofmann, M. & Marko, L. 2014. The Cadomian Orogen:
663 Neoproterozoic to Early Cambrian crustal growth and orogenic zoning along the periphery
664 of the West African Craton – Constraints from U-Pb zircon ages and Hf isotopes
665 (Schwarzburg Antiform, Germany). *Precambrian Research*, **244**, 236-278
666

667 Martínez Catalán, J.R. 2011. Are the oroclines of the Variscan belt related to late Variscan
668 strike-slip tectonics? *Terra Nova*, **23**, 241-247.
669

670 Martínez Catalán, J.R., Arenas, R., Díaz García, F., González Cuadra, P., Gómez-Barreiro,
671 J., Abati, J., Castiñeiras, P., Fernández-Suárez, J., Sánchez Martínez, S., Andonaegui,
672 P., González Clavijo, E., Díez Montes, A., Rubio Pascual F.J. & Valle Aguado, B. 2007.
673 Space and time in the tectonic evolution of the northwestern Iberian Massif: Implications
674 for the Variscan belt. *In*: Hatcher, R.D., Jr., Carlson, M.P., McBride, J.H. and Martínez
675 Catalán, J.R. (Eds.) *4-D Framework of Continental Crust. Geological Society of America*
676 *Memoir*, **200**, 403-423.
677

678 Martínez Catalán, J.R., Arenas, R., Abati, J., Sánchez Martínez, S., Díaz García, F.,
679 Fernández-Suárez, J., González Cuadra, P., Castiñeiras, P., Gómez Barreiro, J., Díez
680 Montes, A., González Clavijo, E., Rubio Pascual, F.J., Andonaegui, P., Jeffries, T.E.,
681 Alcock, J.E., Díez Fernández, R. & López Carmona, A. 2009. A rootless suture and the
682 loss of the roots of a mountain chain: The Variscan belt of NW Iberia. *Comptes Rendus*
683 *Geoscience*, **341**, 114-126.
684

685 Martínez Catalán, J.R., Collett, S., Schulmann, K., Aleksandrowski, P. & Mazur, S. 2020.
686 Correlation of allochthonous terranes and major tectonostratigraphic domains between
687 NW Iberia and the Bohemian Massif, European Variscan belt. *International Journal of*
688 *Earth Sciences*, doi.org/10.1007/s00531-019-01800-z. In press.

689

690 Merinero, R., Lunar, R., Ortega, L., Piña, R., Monterrubio, S. & Gervilla, F. 2013.
691 Hydrothermal palladium enrichment in podiform chromitites of Calzadilla de los Barros
692 (SW Iberian Peninsula). *Canadian Mineralogist*, **51**, 387-404.

693

694 Michard, A., Soulaïmani, A., Hoepffner, C., Ouanaimi, H., Baidder, L., Rjimati, E.C. &
695 Saddiqi, O. 2010. The South-Western Branch of the Variscan Belt: Evidence from
696 Morocco. *Tectonophysics*, **492**, 1-24.

697

698 Mitchell, R.N., Spencer, C.J., Kirscher, U., He, X.-F., Murphy, J.B., Li, Z.-X. & Collins, W. In
699 press. Harmonic hierarchy of mantle and lithospheric convective cycles: Time series
700 analyses of hafnium isotopes of zircon. *Gondwana Research*.

701

702 Nance, R.D., Gutiérrez-Alonso, G., Keppi, J.D., Linnemann, U., Murphy, J.B., Quesada, C.,
703 Strachan, R.A. & Woodcock, N.H. 2010. Evolution of the Rheic Ocean. *Gondwana*
704 *Research*, **17**, 194-222.

705

706 Pearce, J.A. 1996. A user's guide to basalt discrimination diagram. *Geological Association*
707 *of Canada Special Publication*, **12**, 79-113.

708

709 Pearce, J.A. 2008. Geochemical fingerprinting of oceanic basalts with applications to
710 ophiolite classification and the search for Archean oceanic crust. *Lithos*, **100**, 14-48.

711

712 Pearce, J.A. 2014. Immobile element fingerprinting of ophiolites. *Elements*, **10**, 101-108.

713

714 Pearce, J.A. & Cann, J.R. 1971. Ophiolite origin investigated by discriminant analysis using
715 Ti, Zr and Y. *Earth and Planetary Science Letters*, **12**, 339-349.

716

717 Pereira, M.F., Linnemann, U., Hofmann, M., Medina, J. & Silva, J.B. 2012. The provenance
718 of Late Ediacaran and Early Ordovician siliciclastic rocks in the Southwest Central Iberian
719 Zone: Constraints from detrital zircon data on northern Gondwana margin evolution during
720 the late Neoproterozoic. *Precambrian Research*, **192-195**, 166-189.

721

722 Peucat, J.J., Bernard-Griffiths, J., Gil Ibarguchi, J.I., Dallmeyer, R.D., Menot, R.P., Cornichet,
723 J. & Iglesias Ponce de León, M. 1990. Geochemical and geochronological cross section
724 of the deep Variscan crust: The Cabo Ortegal high-pressure nappe (northwestern Spain).
725 *Tectonophysics*, **177**, 263-292.

726

727 Richter, F.M. 1973. Dynamical models for sea floor spreading. *Reviews of Geophysics*, **11**,
728 223-287

729

730 Rojo-Pérez, E., Arenas, R., Fuenlabrada, J.M., Sánchez Martínez, S., Martín Parra, L.M.,
731 Matas, J., Pieren, A.P. & Díez Fernández, R. 2019. Contrasting isotopic sources (Sm-Nd)
732 of Late Ediacaran series in the Iberian Massif: Implications for the Central Iberian-Ossa
733 Morena boundary. *Precambrian Research*, **324**, 194-207.

734

735 Sánchez Martínez, S., Arenas, R., Díaz García, F., Martínez Catalán, J.R., Gómez Barreiro,
736 J. & Pearce, J. 2007. The Careón Ophiolite, NW Spain: supra-subduction zone setting for
737 the youngest Rheic Ocean floor. *Geology*, **35**, 53-56.

738

739 Sánchez Martínez, S., Arenas, R., Gerdes, A., Castiñeiras, P., Potrel, A. & Fernández-
740 Suárez, J. 2011. Isotope geochemistry and revised geochronology of the Purrido Ophiolite

741 (Cabo Ortegal Complex, NW Iberian Massif): Devonian magmatism with mixed sources
742 and involved Mesoproterozoic basement. *Journal of the Geological Society, London*, **168**,
743 733-750.

744

745 Sánchez Martínez. S., Gerdes, A., Arenas, R. & Abati, J. 2012. The Bazar Ophiolite of NW
746 Iberia: a relict of the Iapetus-Tornquist Ocean in the Variscan suture. *Terra Nova*, **24**, 283-
747 294.

748

749 Sánchez Martínez, S., Arenas, R., Albert, R., Gerdes, A. & Fernández-Suárez, J. 2020.
750 Updated geochronology and isotope geochemistry of the Vila de Cruces Ophiolite: A case
751 study of a peri-Gondwanan back-arc ophiolite. *Geological Society, London, Special*
752 *Publications*. In press.

753

754

755 Shervais, J.W. 1982. Ti-V plots and the petrogenesis of modern and ophiolitic lavas. *Earth*
756 *and Planetary Science Letters*, **59**, 101-118.

757

758 Soulimani, A., Ouanaimi, H., Michard, A., Montero, P., Bea, F., Corsini, M., Molina, J.-F.,
759 Rjijmati, E.-C., Saddiqi, O. & Hefferan, K. 2019. Quartzite crests in Paleoproterozoic
760 granites (Anti-Atlas, Morocco); a hint to Pan-African deformation of the West African
761 Craton margin. *Journal of African Earth Sciences*, **157**, 103501.

762

763 Stampfli, G.M., Hochard, C., Vérard, C., Wilhem, C. & von Raumer, J. 2013. The formation of
764 Pangea. *Tectonophysics*, **593**, 1-19.

765

766 Torsvik, T.H. 2003. The Rodinia jigsaw puzzle. *Science*, **300**, 1379-1381.

767

768 Vermeesch, P. 2012. On the visualisation of detrital age distributions. *Chemical Geology*,
769 **312**, 190-194.

770

771 Weil, A.B., Gutiérrez-Alonso, G., Johnston, S.T. & Pastor-Galán, D. 2013. Kinematic
772 constraints on buckling a lithospheric-scale orocline along the northern margin of
773 Gondwana: A geologic synthesis. *Tectonophysics*, **582**, 25-49.

774

775

776 **Figure captions**

777

778 **Fig. 1.** Reconstruction of a part of Pangea at the end of the Paleozoic with the distribution of
779 orogens in the Baltica-Laurentia-Avalonia-Gondwana junction. The general structure and
780 domains of the Variscan Orogen is shown, as well as the location of the ophiolites
781 described in this work (stars): 1) Bou Azzer Ophiolite; 2) Calzadilla Ophiolite; 3) Villa de
782 Cruces Ophiolite; 4) Bazar Ophiolite; 5) Careón Ophiolite; 6) Purrido Ophiolite; 7) Moeche
783 Ophiolite. Pangea map based on Martínez Catalán et al. (2009) and Díez Fernández and
784 Arenas (2015).

785

786 **Fig. 2.** General map of the Anti-Atlas Domain showing the location of the Neoproterozoic
787 Bou Azzer Ophiolite. This region represents the northern boundary of the West African
788 Craton. Several tectonic windows or inliers contain Paleoproterozoic (2200-2000 Ma) to
789 Late Ediacaran formations, which occur below unconformable thick Paleozoic series
790 (Michard et al., 2010; Brahimy et al., 2018; Soulaïmani et al., 2019). The eastern part of
791 the Anti-Atlas Domain is affected by Variscan deformation that developed a generation of
792 large folds with axial traces trending NE-SW. Modified after Michard et al. (2010).

793

794 **Fig. 3.** Terrane distribution and geotectonic zones in the Iberian Massif (Díez Fernández and
795 Arenas, 2015; Arenas et al., 2016b), and location of the Neoproterozoic and Paleozoic

796 ophiolites described in this work. Abbreviations: AF, Azuaga Fault; BAO, Beja-Acebuches
797 Ophiolite; CA, Carvalhal Amphibolites; CF, Canaleja Fault; CMU, Cubito-Moura Unit;
798 BCU, Badajoz-Córdoba Unit; ET, Espina Thrust; HF, Hornachos Fault; IOMZO, Internal
799 Ossa-Morena Zone Ophiolites; LLF, Llanos Fault; MLF, Malpica-Lamego Fault; OF, Onza
800 Fault; OVD, Obejo-Valsequillo Domain; PG-CVD, Puente Génave-Castelo de Vide
801 Detachment; PRF, Palas de Rei Fault; PTF, Porto-Tomar Fault; RF, Riás Fault; VF,
802 Viveiro Fault.

803

804 **Fig. 4.** Representative schematic columns for some of the Neoproterozoic and Paleozoic
805 ophiolites of the Moroccan Anti-Atlas and the Iberian Massif.

806

807 **Fig. 5.** Hf isotope evolution diagram showing combined U-Pb and Lu-Hf data of all available
808 zircon analyses in the described ophiolites. $\epsilon_{\text{Hf}(t)}$ values were considered close DM for the
809 c. 700 Ma Bou Azzer Ophiolite, as isotopic Hf analyses in zircon have not been published.
810 Oblique colored bands represent crustal evolution trends for Eburnean and Cadomian DM
811 derived rocks. Adaptive Kernel Density Estimation of analyzed zircon with Lu-Hf
812 systematics is represented in grey, with binwidth of histograms built at 20 Ma (Density
813 Plotter5.0 software; Vermeesch, 2012). CHUR, chondritic uniform reservoir; DM, depleted
814 mantle; MORB, mid-ocean ridge basalt. DM, MORB and crustal trends were calculated as
815 described by Albert et al, 2015.

816

817 **Fig. 6.** Th/Yb versus Nb/Yb diagram (Pearce 2008, 2014) for the ophiolites described in this
818 work (geochemical data from 117 mafic samples). This diagram allows differentiate the
819 tectonic settings in which the ophiolites were generated. The compositions of mid-ocean
820 ridge ophiolites follow the N-MORB-OIB array. However, supra-subduction zone ophiolites
821 are distributed above this array in the regions where oceanic or continental arcs
822 compositions are represented.

823

824 **Fig. 7.** Ti-V plot (Shervais, 1982; Pearce, 2014) for the composition of the ophiolites
825 described in the text (n = 117). This diagram is used to differentiate mid-ocean ridge
826 basalts (MORB), island arc tholeiites (IAT) and boninite magma types. However, used
827 after the previous Th/Yb versus Nb/Yb diagram (Fig. 6), once the existence of MORB
828 compositions has been ruled out, this diagram allows to recognize the composition of
829 back-arc basin or fore-arc basin basalts (BABB and FAB) generated in slab-proximal or
830 slab-distal settings.

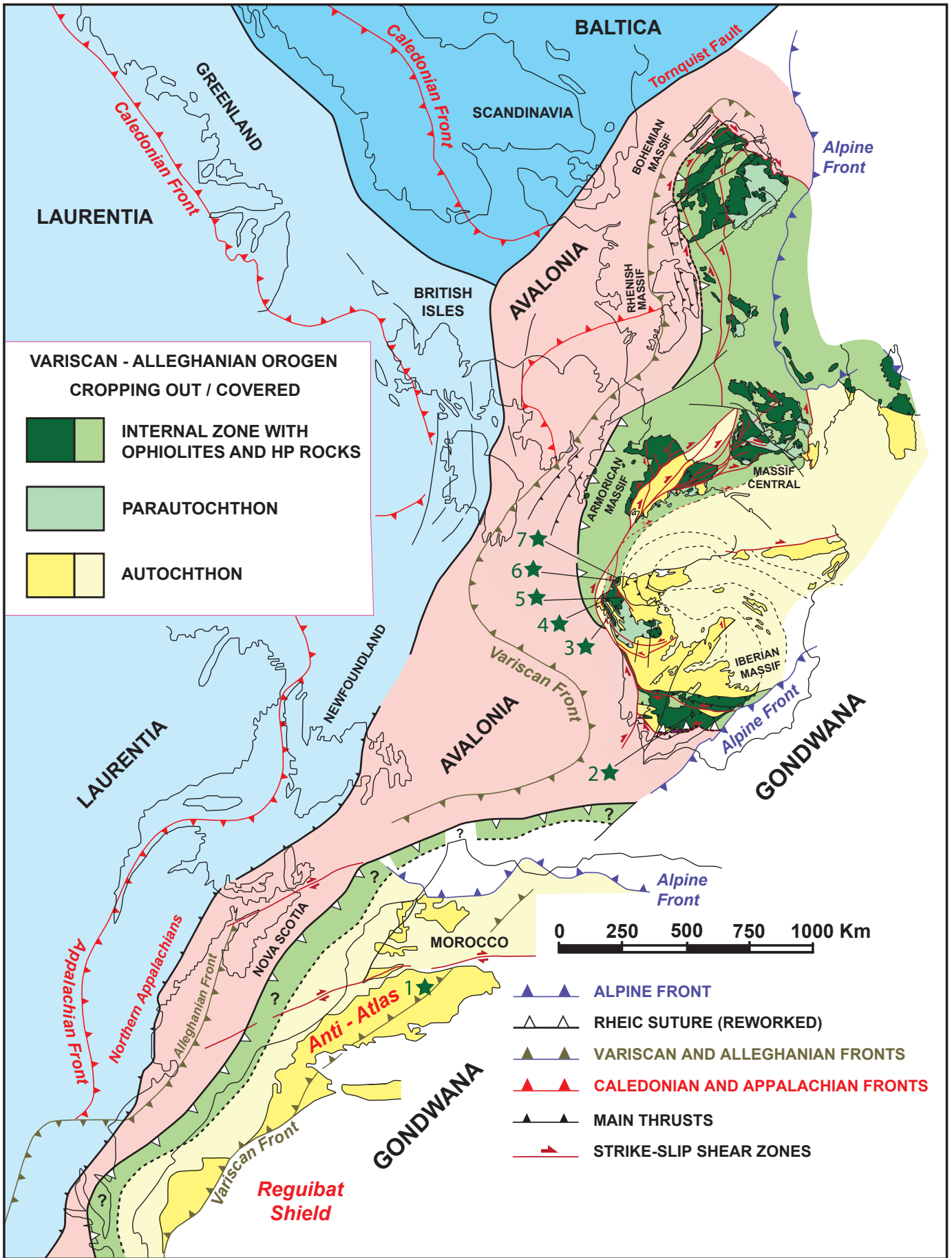
831

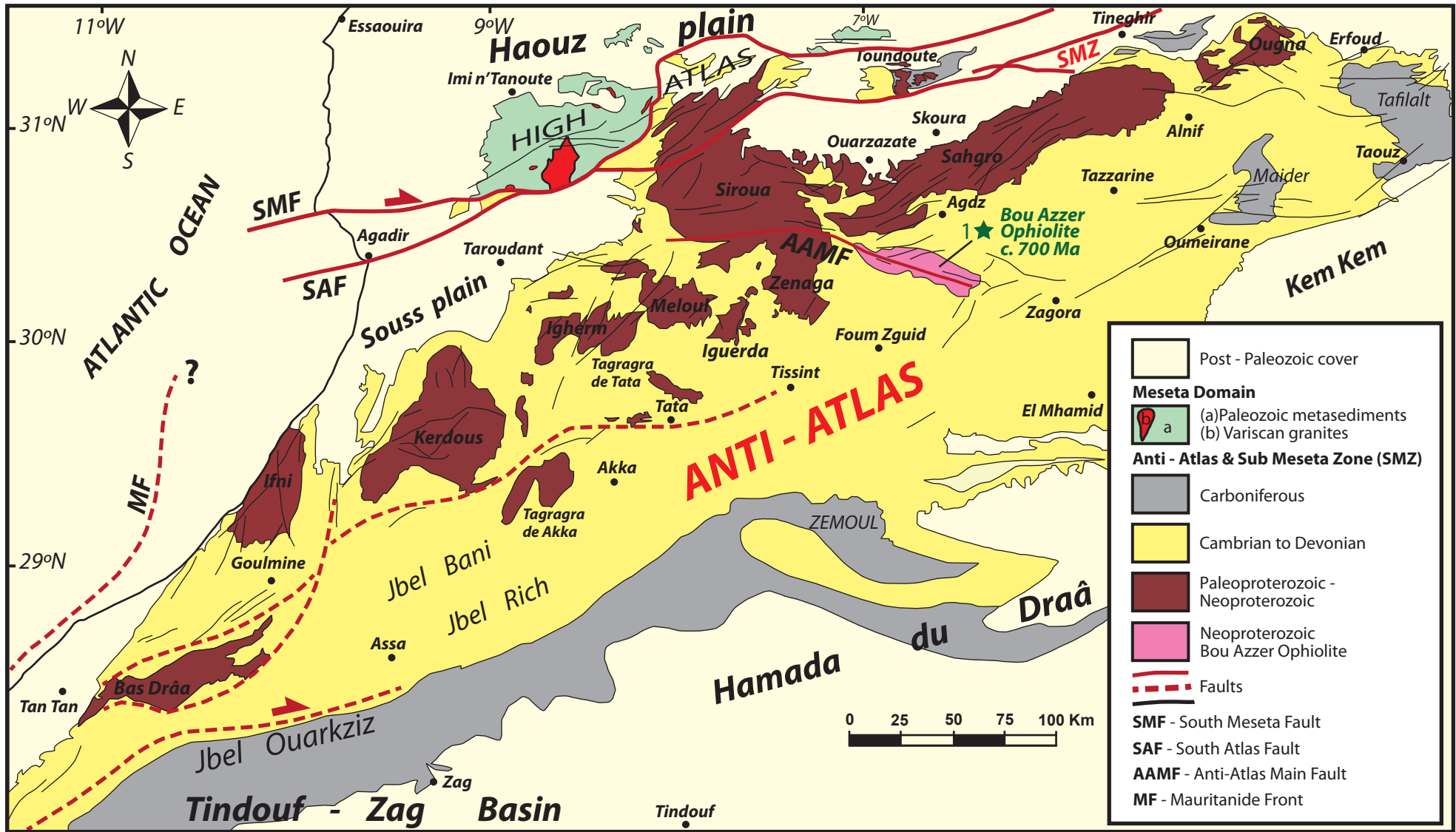
832 **Fig. 8.** Paleogeographic context in the periphery of NW African-Iberian Gondwana and proto-
833 Gondwana between c. 700 Ma and c. 500 Ma. A) Opening of the Reguibat fore-arc basin
834 above the associated Reguibat trench, in the western branch of the Pharusian Ocean
835 (Stampfli et al., 2013). The Reguibat fore-arc basin is considered the dynamic setting for
836 the generation of the mafic protoliths of the Bou Azzer Ophiolite. B) Obduction of the Bou
837 Azzer Ophiolite at c. 653-640 Ma (El Hadi et al., 2010) occurred during the closure of the
838 Pharusian Ocean and the development of the Trans Saharan Orogen (Brahimi et al.,
839 2018). This Pan-African Orogen is part of the complex interactions between crustal blocks
840 that finally assembled Gondwana at c. 600 Ma. In the NW African-Iberian margin of
841 Gondwana, subduction of the lithosphere of the Panafrican Ocean probably caused the
842 development of a long Cadomian fore-arc basin, associated with the long well-dated peri-
843 Gondwanan volcanic arc (Linnemann et al., 2014; Albert et al., 2015). This fore-arc basin
844 is considered the dynamic context where the protoliths of the Calzadilla Ophiolite were
845 generated. C) Obduction of the Calzadilla Ophiolite in the Ediacaran–Early Cambrian
846 boundary occurred during complex interaction between the fore-arc basin and the volcanic
847 arc (Arenas et al., 2018; Díez Fernández et al., 2019). Later on, at c. 500 Ma, a back-arc
848 basin opened along the external margin of Gondwana pulling away sections of the
849 volcanic arc, still active for some time in both sides of this basin (Arenas et al., 2007).
850 Generation of this back-arc basin was associated with the pronounced extensional event
851 that affected the peri-Gondwana domain, which finally caused the rifting of the Avalonian

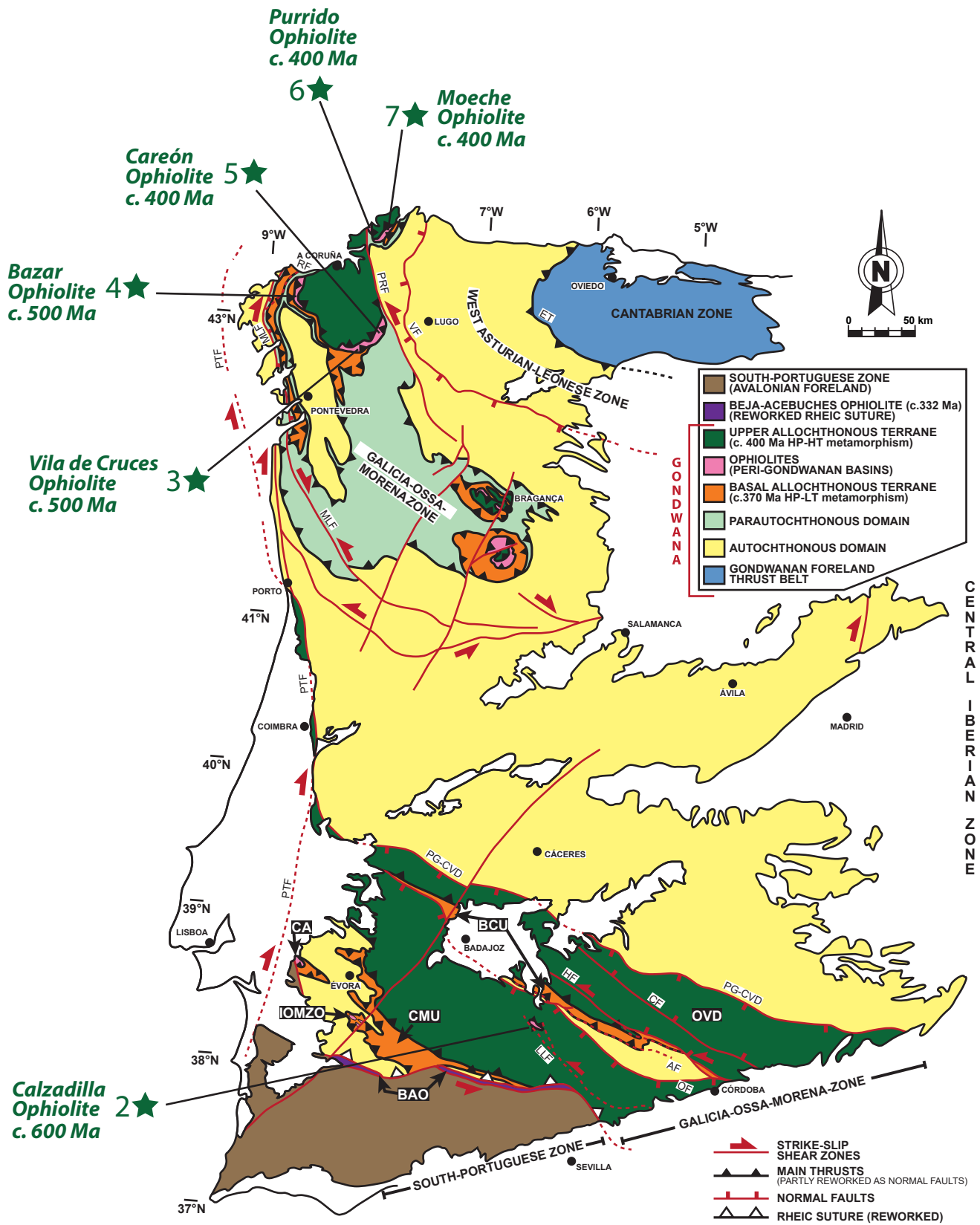
852 terrane and the opening of the Rheic Ocean (Nance et al., 2010). The protoliths of the Vila
853 de Cruces Ophiolite represent the oceanic or transitional lithosphere generated in this
854 back-arc basin.

855

856 **Fig. 9.** Highly schematic reconstruction of the Anti Atlas–Iberia domain showing the probable
857 distribution of the peri-Gondwanan ophiolites at the beginning of the Variscan
858 deformation. The ophiolites dated at c. 400 Ma represent an ephemeral intraorogenic
859 basin opened at c. 395 Ma and shortly accreted to the early Variscan orogenic wedge at
860 c. 385–380 Ma (Arenas et al., 2014a; Díez Fernández et al., 2020). The back-arc basin
861 represented by the Vila de Cruces Ophiolite was affected later by the advancing
862 deformation and its lithologies were incorporated to the orogenic wedge in a lower position
863 (Arenas et al., 2016a; Díez Fernández et al., 2016). Continuity of the ophiolites in the
864 intermediate section between Avalonia and the Anti Atlas is speculative as the most
865 internal Variscan domain is actually submerged in this region. However the westward
866 continuation of the most deformed sectors of the Variscan Orogen, those including
867 ophiolites and high-P units, can be expected according to the position of the boundary
868 between Avalonia and the margin of Gondwana. This boundary represents the Rheic
869 Ocean Suture. The origin of the described ophiolites, all of them derived from long fore-
870 arc or back-arc basins, suggests that its initial geometry in the Variscan Orogen should
871 correspond to units with significant extent along the strike of the Gondwana margin. These
872 ophiolitic units were accreted to the orogenic wedge in between others continental
873 terranes which represent different sections of the Gondwana margin. The location of the
874 Visean Beja-Acebuches Ophiolite in SW Iberia is also shown. The position of Iberia,
875 British Isles and Anti Atlas is only a reference and does not represent their exact location
876 at the end of the Pangea assembly (Variscan Orogeny in this region).

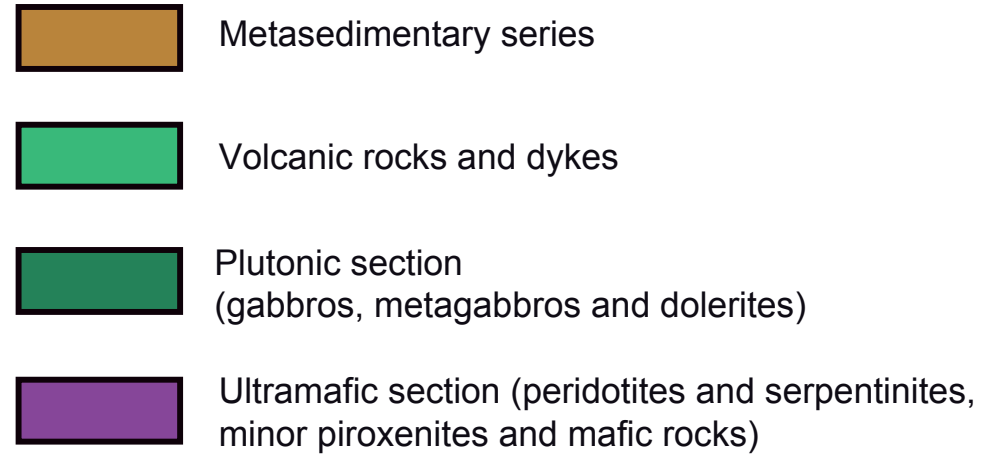
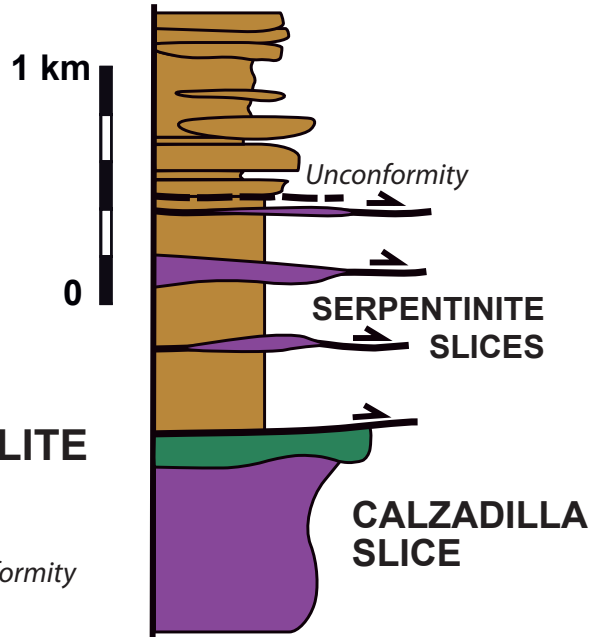




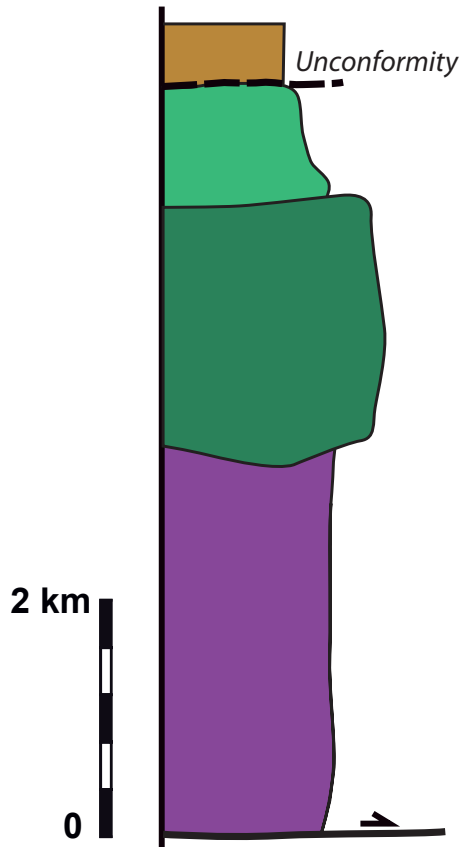


PERI-GONDWANAN OPHIOLITES

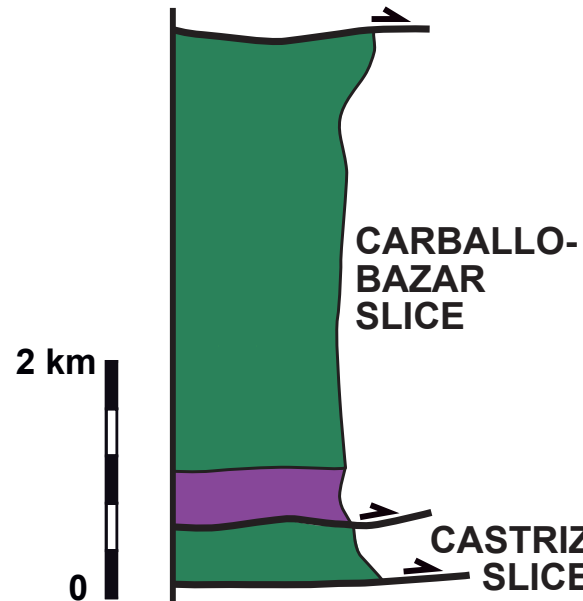
CALZADILLA OPHIOLITE c. 600 Ma



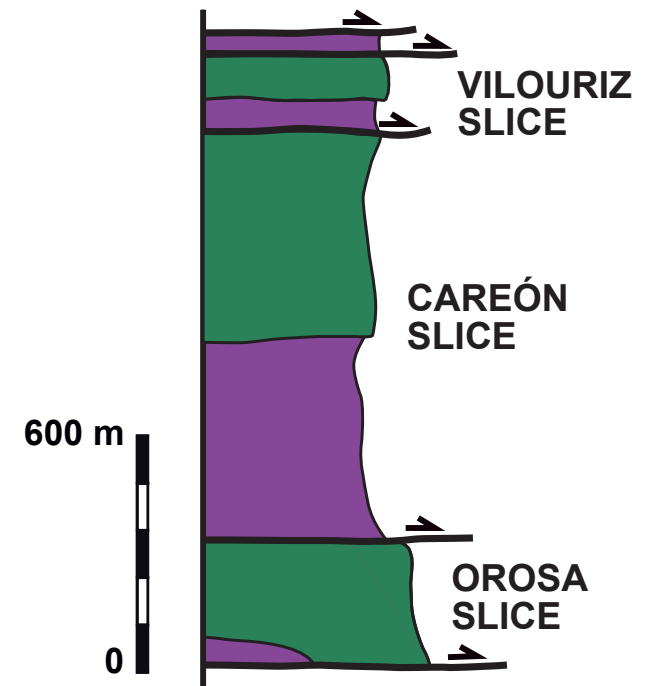
BOU AZZER OPHIOLITE c. 700 Ma



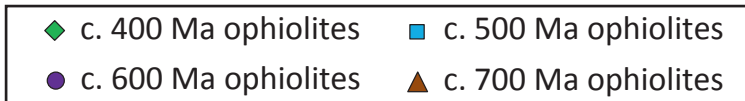
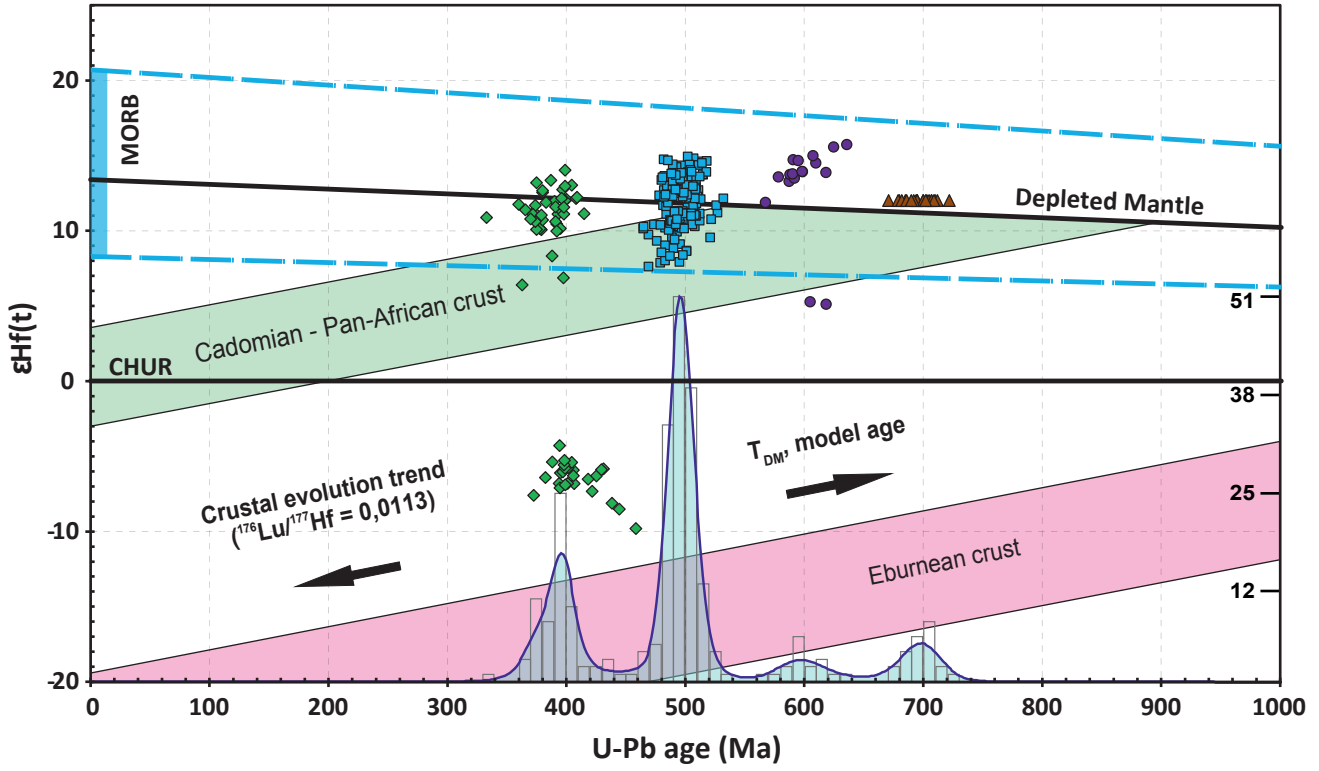
BAZAR OPHIOLITE c. 500 Ma

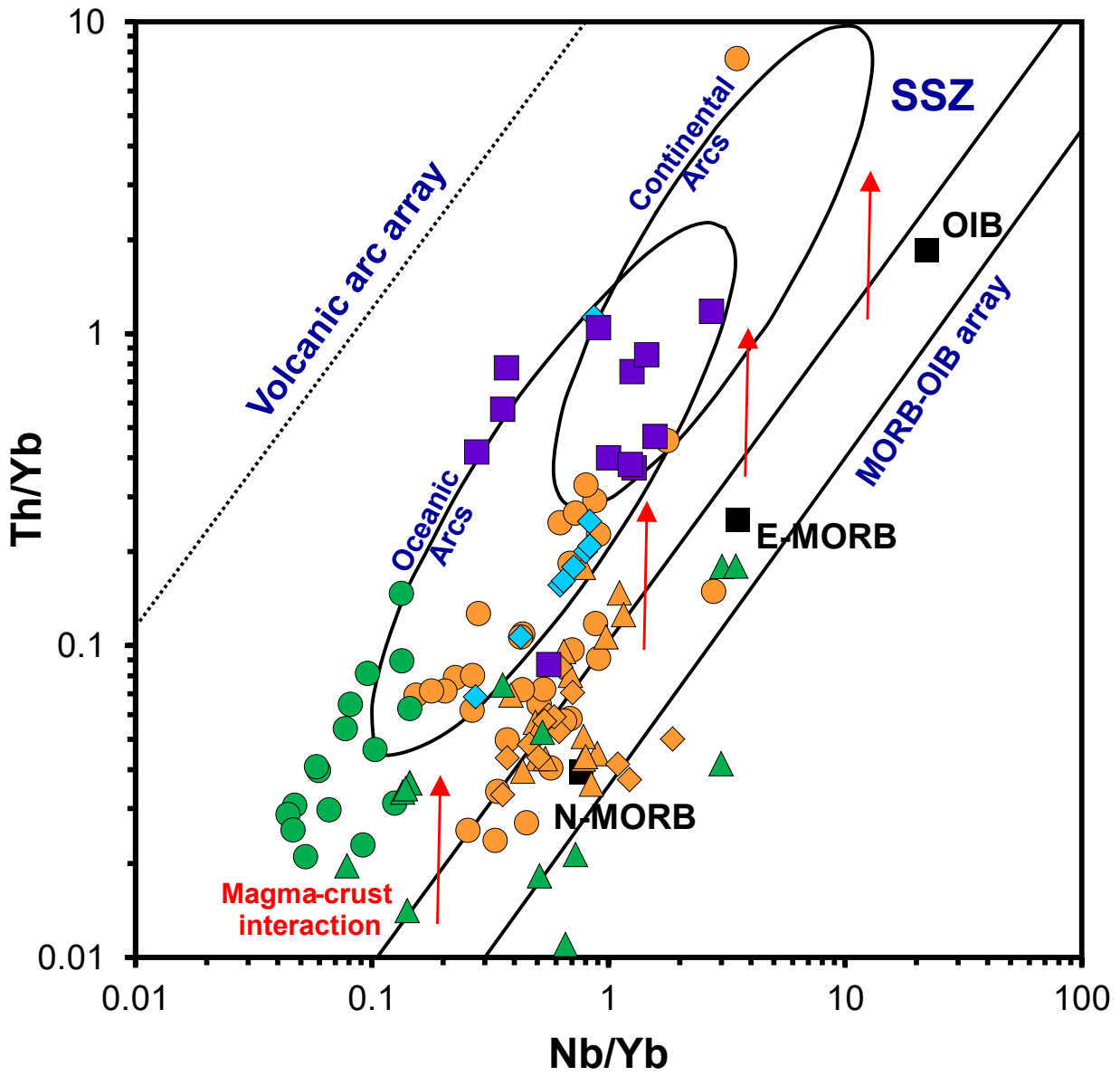


CAREÓN OPHIOLITE c. 400 Ma

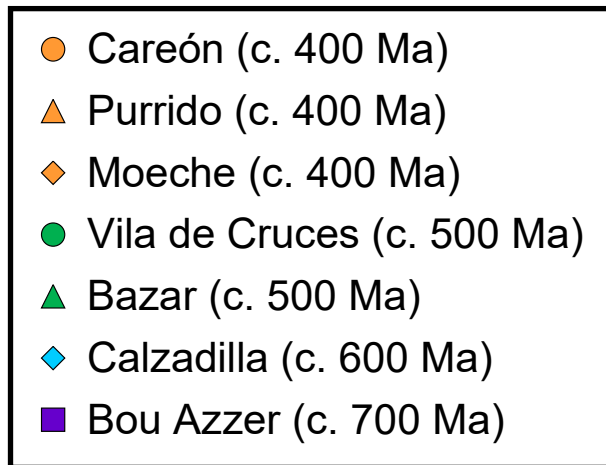
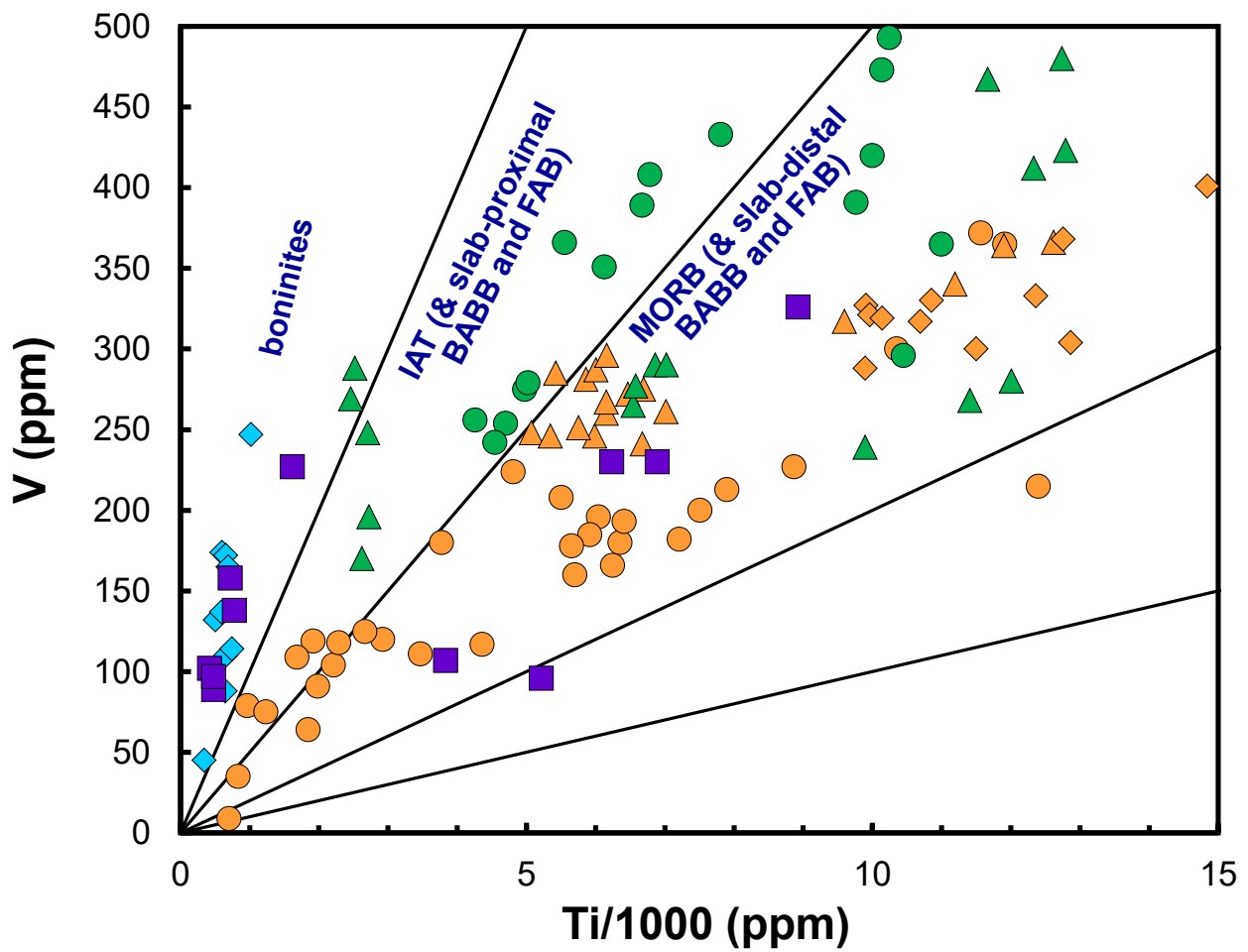


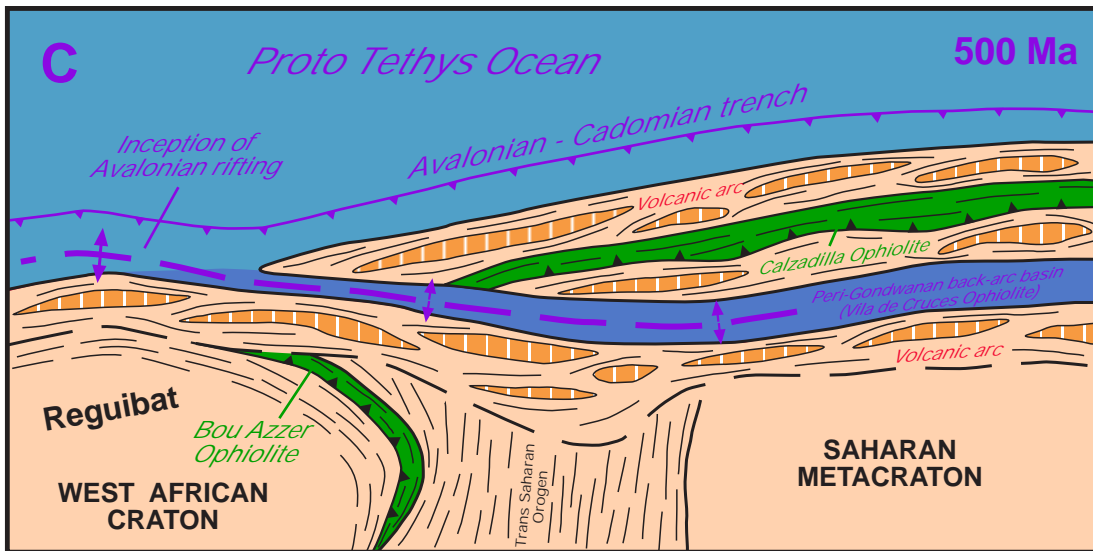
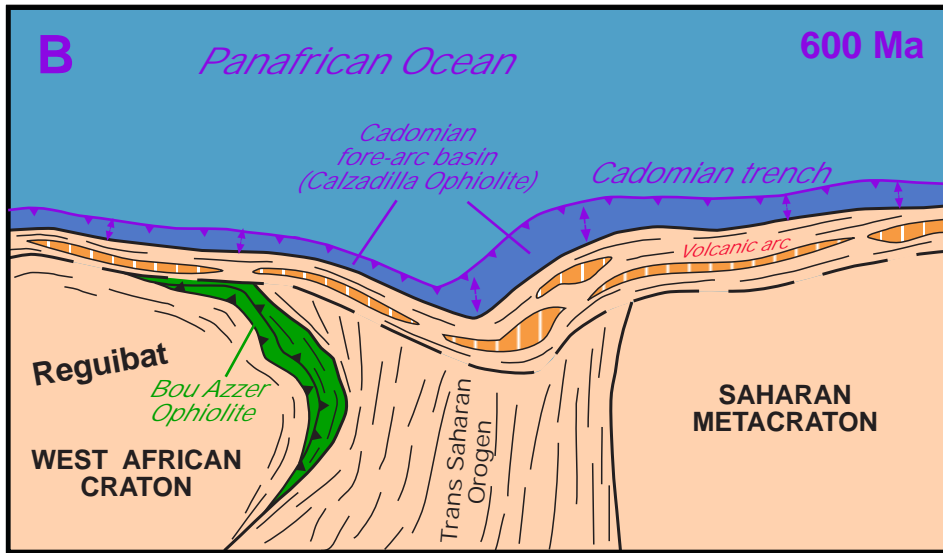
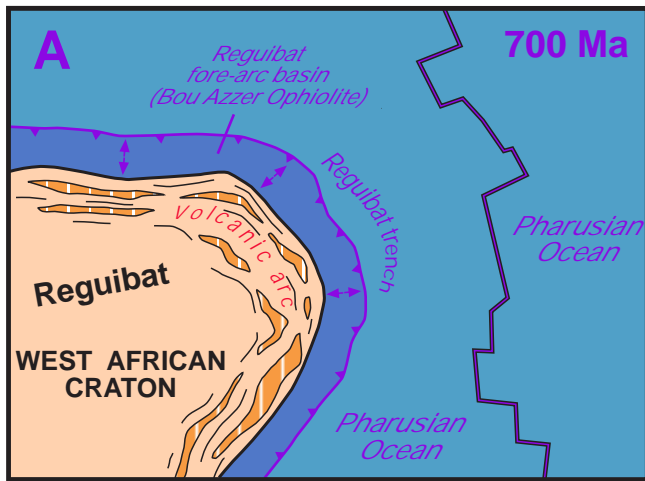
All ophiolites (n=258)





- Careón (c. 400 Ma)
- △ Purrido (c. 400 Ma)
- ◇ Moeche (c. 400 Ma)
- Vila de Cruces (c. 500 Ma)
- ▲ Bazar (c. 500 Ma)
- ◆ Calzadilla (c. 600 Ma)
- Bou Azzer (c. 700 Ma)





OPHIOLITES



VOLCANIC ARCS



FORE-ARC & BACK-ARC BASINS



CONTINENTS



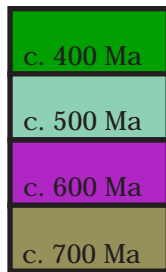
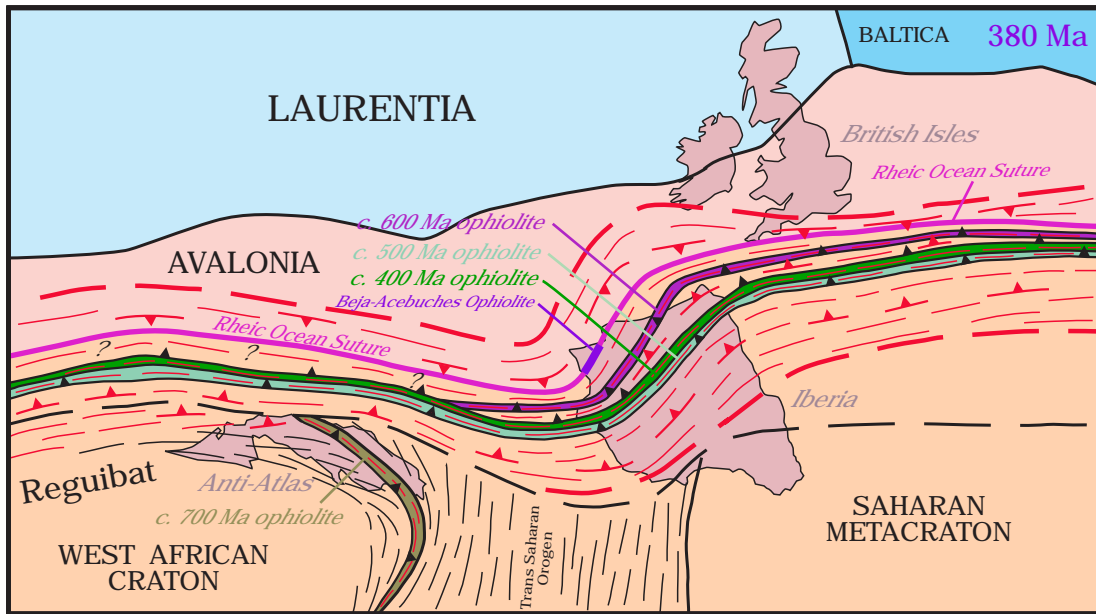
OCEANS



Trenches & ridges



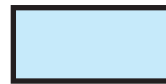
Tectonic trends



OPHIOLITES



AVALONIA



LAURENTIA



BALTICA



GONDWANA



Variscan trends